J Indian Inst Sci, Sept.–Oct. 1996, 76, 639–649

Laser in the study of an ohmically heated jet

G. S. BHAT
Centre for Atmospheric and Oceanic Sciences, Indian Institute of Science, Bangalore 560 012, India.

Received on February 3, 1995; Revised on August 7, 1995.

Abstract

A study of an axisymmetric vertical jet subjected to local volumetric heating is reported. Using flow visualization, digital image processing and laser Doppler techniques, the properties of the jet, namely, the axial component of velocity and scalar length scale have been studied in detail. The jet vortical structure gets disrupted on heating and the jet no longer grows linearly with height, and the normalized turbulence intensity shows a rapid decrease in the region of heating. This study shows that the behaviour of a volumetrically heated jet is markedly different from that of ordinary jets, plumes and buoyant jets.

Keywords: Free shear flow, jet, plume, LDV, flow visualization.

1. Introduction

Taylor's lateral entrainment hypothesis, which has been successfully applied to a variety of free shear flows[1], has not met with much success in the case of cumulus clouds[2]. *In-situ* measurements carried out using instrumented aircraft suggest that some air ascends in clouds almost undiluted, *i.e.*, there is very little entrainment of environmental air and mixing in some regions within a cloud as it grows[3,4]. The physical mechanism responsible for the reduced entrainment in clouds has not been understood. One possibility is that flows in clouds differ from other free shear flows like jets, plumes and thermals because of the release of latent heat due to condensation of water vapour resulting in a local increase in buoyancy. The consequences of such local buoyancy increase on the flow development have not been well understood. The present experiments were undertaken to improve our understanding of flows with (local) buoyancy increase, such as those involving chemical reactions (*e.g.*, combustion) or latent heat release as in clouds. A novel method of ohmically injecting heat into a liquid flow was developed for this purpose[5]. Here the behaviour of the ohmically heated jet is briefly described using laser-based flow visualization and velocity measurement techniques. More details on the fluid dynamic aspects can be found in Elavarasan *et al.*[6], and Bhat and Narasimha[7].

The paper is organized as follows. Section 2 contains a brief description of the flow and Section 3 the experimental arrangement including the method of heating adopted. Section 4 presents representative results followed by conclusions in Section 5.

2. Locally heated jet

A schematic of the flow configuration is given in Fig. 1. The flow is basically an axisymmetric vertical jet till it reaches the height $z = z_b$. Heat is volumetrically added in the

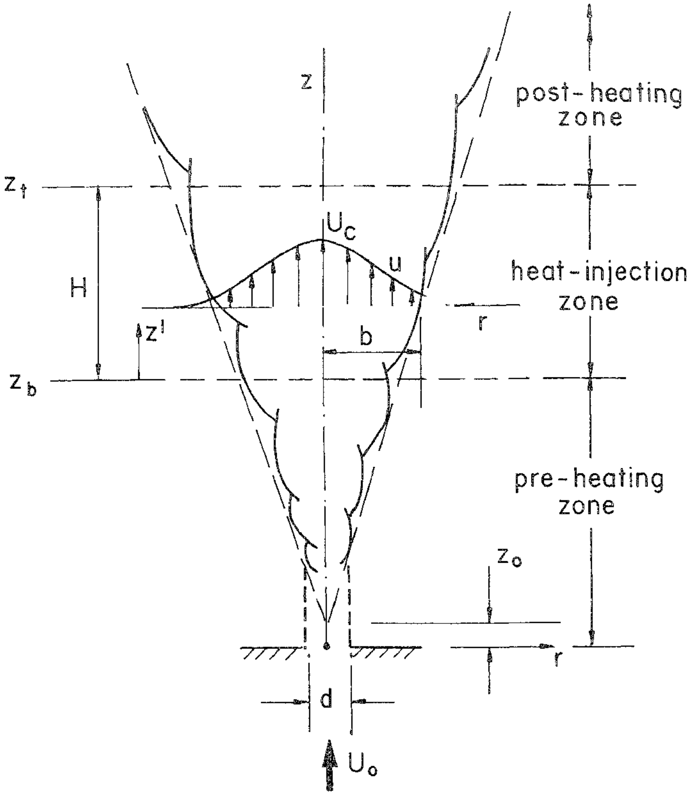

FIG. 1. A schematic of the flow configuration. For $z < z_b$, the flow is an axisymmetric vertical jet and is heated in the region $z_b < z < z_t$ by selectively making the jet fluid electrically conducting and applying a high-frequency voltage across the electrodes placed in this region.

region $z_b < z < z_t$. The buoyancy flux (weight deficit per unit time), which is proportional to the increase in temperature ΔT of the jet fluid, increases from zero at $z = z_b$ to a maximum value at $z = z_t$. For $z > z_t$, the net buoyancy flux remains constant.

For convenience, the following nomenclature has been used to refer to different regions of the jet. The neutral jet region, *i.e.*, $z < z_b$, will be called the pre-heating zone, the region $z_b < z < z_t$ in which heat is added to the flow is the heat-injection zone and the region above this is the post-heating zone.

In the experiments, z_b/d was large (≥ 25) so that buoyancy comes into play only after the jet has reached approximate equilibrium (self-similarity) which is disturbed by heating. A consequence of this is that profiles of mean temperature and mean axial velocity across the jet need not be similar amongst themselves or related to each other. This is in contrast to developed jets and plumes, where the scalar and velocity length scales are related, and their profiles across the jet are similar[8].

3. Experimental arrangement

3.1. *Basic set-up*

Details of the basic experimental arrangement and the method of heating are given in Bhat *et al.*[5] and Elavarasan *et al.*[6]; here the arrangement is described briefly (Fig. 2). Experiments were carried out in a glass tank of dimension 60 × 60 × 120 cm (height). The tank was filled with filtered and deionised water and the jet entered from the bottom through an 8-mm dia nozzle after undergoing an area contraction of 25. In some

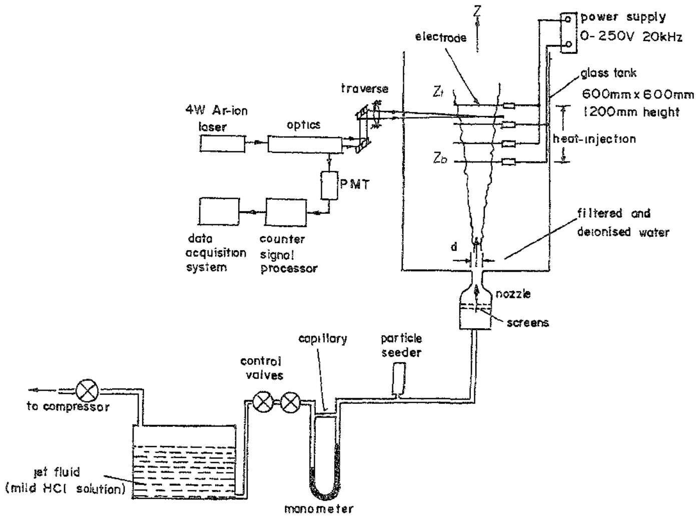

FIG. 2. A schematic of the experimental arrangement.

experiments, a suitably designed cap was fitted inside the nozzle so that the diameter of the nozzle at the exit was 1.5 mm. In the experiments, z_b was 200 mm so that $z_b/d = 25$ or 133, and this large value ensured that the jet was fully developed before being subjected to heating.

Volumetric heating of the jet fluid was carried out by selectively rendering it electrically conductive and applying a high-frequency (20 kHz) AC voltage between electrodes placed horizontally across the flow at desired heights. Electrical conductivity was obtained by adding a small quantity of HCl (~2 ml/l of water) to the jet fluid, the resulting increase in density being neutralized by adding an appropriate amount of acetone. Electrodes were made of fine platinum wire (0.09 mm dia.) netted on a rectangular supporting frame whose inside open area was 200 × 200 mm. It was found necessary to place more than two electrodes in the flow for injecting adequate quantities of heat into the jet: in the experiments reported here five electrodes were used with alternate ones connected in parallel. The amount of heating was easily controlled by varying the voltage across the electrodes, but the maximum was limited to about 1200 W, as, at higher heating rates, electrolysis occurs within a few minutes of commencement of heat injection.

3.2. *Flow visualization and recording*

In recent years, the laser-induced fluorescence (LIF) technique has been widely employed to obtain two-dimensional sections of axisymmetric flows[9,10]. The technique has the advantage in that it can reveal the structure of the flow with spatial resolution touching Kolmogorov scales and also facilitates quantitative estimation of dye concentration and spread rates[9,10]. It appeared attractive for the present experiments and has been employed in this study.

A fluorescent dye (Rhodamine 6G) used in the present experiments absorbs light energy in some wavelength range and emits radiation at longer wavelengths, uniformly in all directions[11,12]. The fluorescence intensity I_f received at a suitably located detector is given by[12]

$$I_f = K\,\phi\,\varepsilon\,c(s)\,I_e(s)\,ds \tag{1}$$

where K is the fraction of the available fluorescence light energy collected at the detector, ϕ, the quantum efficiency of the dye, ε, the dye absorptivity or extinction coefficient, c, the dye concentration, I_e, the exciting light intensity, and s, the distance measured in the direction of light propagation. Equation (1) is the basis for quantitative measurements. A linear response between c and I_f is observed for values of c up to about 100 μg/ml, but as the dye concentration increases, a process known as quenching takes place and eqn (1) will not be valid[11]. Another aspect that needs attention in the present study is the observation that with other conditions remaining the same, I_f decreases with increasing temperature; the rate depends on the dye and the solvent; it is about 1% per degree centigrade increase for most dyes[11].

A 4-WAr-ion laser along with a combination of three spherical lenses and a cylindrical lens have been used to produce a laser light sheet with a thickness of about 400 μm

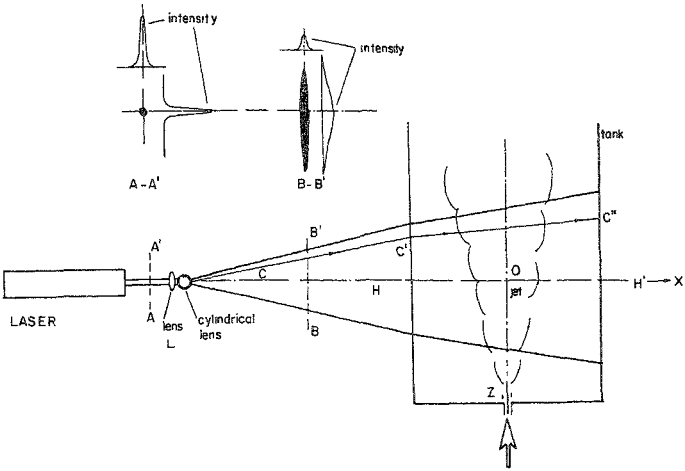

FIG. 3. A schematic of laser sheet illumination arrangement. The circular laser beam (section A–A') spreads into a light sheet (section B–B') after passing through the cylindrical lens.

in the region where the jet sections were taken (Fig. 3). This has been recorded both by still photography and on video.

For calculating the dye concentration width, the video tape was played back on a VCR and the images of the jet sections were fed to an image digitizer. The digitizer unit consisted of a video decoder–encoder board to convert PAL colour signal into RGB signal and *vice versa* (Data Translation, USA, model DT2869) and a colour frame grabber board (model DT2871), both mounted inside an IBM PC/AT 386 system. The digitized colour image is stored in three onboard frame buffers with 512×512 pixel resolution and 8 bit accuracy.

3.3. *Velocity measurements*

The jet velocity varies rapidly across as well as along the jet axis. Theoretical considerations suggest that for heating to be effective, the velocity scale (*i.e.*, the jet centreline velocity) in the heat-injection zone be less than about 0.1 m/s. So, in these experiments, velocities to be measured are in the range zero to a few m/s*. Further, there is a strong electric field in the heat-injection zone and this rules out the use of hot-wire technique

*In an axisymmetric jet, the velocity scale is inversely proportional to the distance from the nozzle exit, and hence in the pre-heating zone velocities can be a few m/s.

for velocity measurements. The laser Doppler technique offers a convenient means of measuring velocity in this flow and has been used here. The principles and techniques of LDV are now well known[13–15]. Basically the technique measures the Doppler shift in the frequency of the scattered light from minute particles suspended in the flow and infers the velocity from this information. The laser beams and light collecting optics can be suitably arranged to measure velocity component along any given direction.

The LDV system used in the present investigation is a two-colour four-beam system (TSI make model No. 9100-7). Seeding is important, for apart from the laser power, scattering property of the particles controls the signal-to-noise ratio. Also, the particles should faithfully follow the flow since flow velocity is inferred from the light scattered by the particles suspended in the flow. In the present measurements, finely ground aluminium powder with a size $<10\,\mu m$ has been used for seeding. The particles were mixed with tank water and stirred well, and then left undisturbed for about two hours before making the measurements to allow large particles to settle down. To improve the measured accuracy, especially that of low velocities, one of the two beams that measures the axial component of velocity is frequency-shifted by 40 MHz using a Bragg cell. Counter-type signal processors have been used and the output from the counters is fed to a data-acquisition system which stores the velocity information on a hard disk that can be analysed afterwards.

4. Results

4.1. *Flow visualization*

Photographs of vertical and horizontal sections of the jet, taken on a Kodak 1600 ASA colour film with an exposure time between two and four milliseconds, are shown in Figs 4 and 5, respectively. In these experiments, the jet inlet velocity is constant (1 m/s) and the heating rate is varied. Figure 4(a) shows an instantaneous vertical section of the unheated jet (the thin horizontal lines in the pictures are due to the supporting frames of the electrode wire grids). The brighter regions contain the (original) jet fluid whereas the darker regions are occupied by the ambient fluid. It is seen that the jet is dominated by large eddies, and the instantaneous structure is far from being smooth. The large eddies seen in Fig.4(a) are basically responsible for turbulent entrainment, *i.e.*, they bring in the ambient fluid into the jet[16,17]. Even in the vicinity of the jet axis there are some dark regions implying the presence of essentially unmixed ambient fluid there. Therefore, the ambient fluid is first dragged into the flow by large eddies and molecular mixing takes place more gradually. The present results are consistent with previous observations[9,17] Further, it may be observed that the presence of electrodes causes no noticeable change in the structure of the jet in this region.

The jet section corresponding to a heating rate of 600 W is shown in Fig. 4(b). The pre-heating zone structure is similar in nature to that seen in Fig. 4(a). In the heat-injection zone, the eddies are not as sharply defined, the horizontal extent of the large eddies has diminished, and the lateral growth of the jet has reduced. To sum up, the jet eddy structure has been disrupted in the heat-injection zone with a likely consequence on the entrainment of the ambient fluid into the jet.

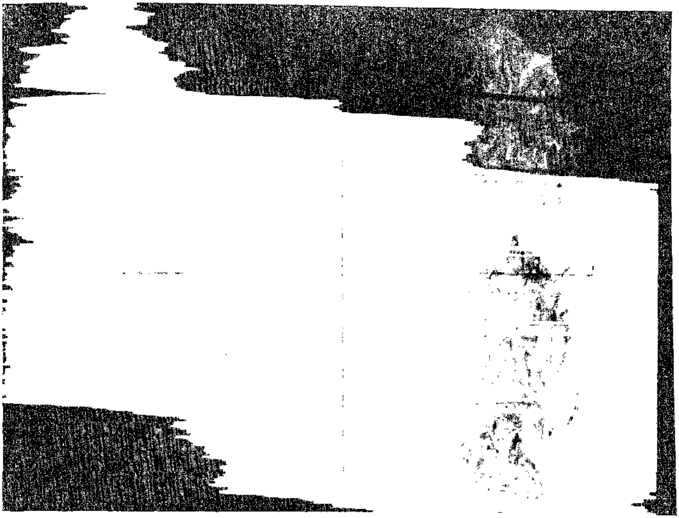

(a) (b)
FIG. 4. Vertical sections through the jet at an jet inlet velocity of 1 m/s (a) unheated jet, (b) heated jet, $Q = 600$ W.

The change in the structure of the jet with heating is seen in the horizontal sections as well. Figure 5(a) shows a section through the unheated jet at $z = 305$ mm, a location

(a) (b)
FIG. 5. Horizontal sections taken at $z = 300$ mm. (a) unheated jet, and (b) heated jet $Q = 600$ W.

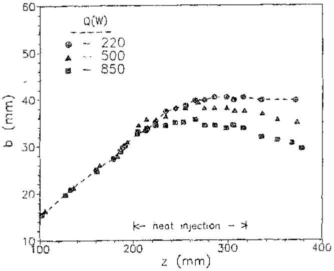

FIG 6. Dependence of jet scalar width b on heating rate Q.

mid-way between the top two grids. The instantaneous structure is far from being axi-symmetric and the jet boundary, as defined by the dye, is rather sharp. A horizontal section taken at $Q = 600$ W is shown in Fig. 5(b). Here it is difficult to identify an eddy clearly and the jet is narrower. The horizontal sections thus confirm that, with increased heating, the jet narrows down and its eddy structure progressively gets more and more obscure.

These pictures show that laser is a very powerful tool in flow visualization and enables insights into flow behaviour which are otherwise impossible. In fact, the two-dimensional sections so taken can be used for obtaining quantitative information using digital image processing. The intensity (brightness) field is proportional to the dye concentration field provided the incident light intensity is known (eqn 1). The latter can be obtained independently for a given optical arrangement. For example, Fig. 6 shows the variation of jet width (distance from jet axis where the dye mean concentration drops to $1/e$ times its value on jet axis) with axial distance for three values of heating keeping the jet inlet velocity constant at 1 m/s. This figure shows that in the pre-heating zone, the jet width is not noticeably affected by volumetric heating and the spread rates are the same for all values of Q. Immediately after entering the heat-injection zone, there is a slight increase in the spread rate which appears to increase with Q. However, soon the jet spread rate begins to decrease and the width of heated jet departs from the unheated jet trend, and over some streamwise distance becomes nearly constant.

4.3. *Axial component of centreline velocity*

Figure 7(a) shows the variation of the axial component of velocity along the jet axis. It is seen that at the highest heating rate and the lowest jet inlet velocity, the jet accelerates slightly in the upper heat-injection and lower post-heating zones. Figure 7(b) shows the normalized turbulence intensity along the jet axis. It is seen that as Q increases, the normalized intensity u'_c/U_c experiences a drastic reduction (by about 35%) in the early part of the heat-injection zone, and thereafter it seems to reach an asymptotic value of

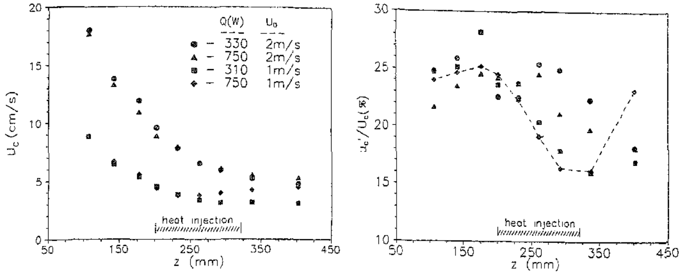

FIG. 7(a). Variation of the axial component of the centreline velocity along the jet axis as a function of Q. (b) Normalized turbulent intensity along the jet axis as a function of Q.

about 16%. The normalized intensity increases again in the post-heating zone for large values of Q, and could be tending towards the equilibrium value in a plume. However, at two lower values of Q, the normalized intensity is still falling, indicating a very slow relaxation. This is consistent with experience in other free shear flows[18].

The distribution of the axial component of velocity across the jet has been measured at a few axial stations, and shows no noticeable change in profile shape with heating (Fig.8(a)). An almost similar behaviour is seen in the dye concentration distribution as well (Fig.8(b)), except that a slight widening of the profile in the post-heating zone is noticeable in this case. A Gaussian distribution describes the shape fairly well in the central region of the jet, and the experimental points generally fall off more rapidly towards the edges of the jet.

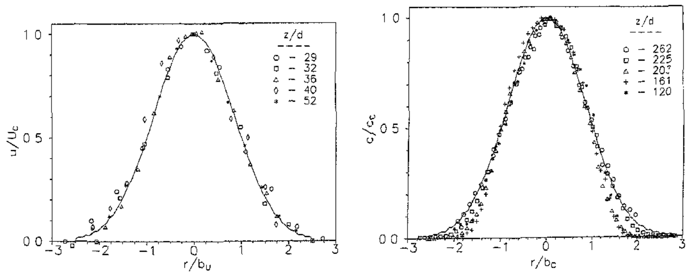

FIG. 8(a). Velocity profiles across the heated jet normalized by the local velocity and length scales. $d = 8$ mm. $Re_0 = 1720$ and $Q = 550$ W. The first four stations are in the heat-injection zone whereas the last one ($z/d = 52$) is in the post-heating zone. The continuous curve is the Gaussian distribution. (b) Distribution of the dye concentration across the heated jet. $d = 1.5$ mm, Re_0 1600, $Q = 700$ W and the heat-injection zone is $133 < z/d < 213$. Please note that half-width is used as length scale for normalizing the radial distance.

5. Conclusions

1. This study demonstrates the usefulness of laser in the study of an ohmically heated jet. The presence of an electric field and low values of flow velocities rule out the use of techniques other than LDV for obtaining mean velocity and turbulence statistics accurately.

2. It is seen that volumetric heating disrupts the jet eddy structure in the heat-injection zone, the jet spread rate reduces drastically, and even visually its behaviour is very different from that of a jet. Since the large eddies responsible for the turbulent entrainment are disrupted, this can lead to reduced entrainment.

3. The decay of the centreline velocity is arrested following volumetric heating. However, it is the normalized turbulent intensity that shows a more dramatic change, decreasing by as much as 35% in the heat-injection zone at high heating rates.

4. The profiles of velocity and dye concentration across the jet do not show any distinct change in shape with heating when normalized by the local scales.

Acknowledgements

This work was partially sponsored by grants from the Department of Science and Technology, New Delhi, and the Extra Mural Division, CSIR, New Delhi. The author appreciates the grants provided and sincerely thank these agencies. Prof. Narasimha has been associated with this work from the very beginning and the author is grateful to him for all encouragement and help received. The author also thanks Dr R. Elavarasan and Mr L. Venkatakrishnan for their assistance in conducting the experiments and LDV measurements, Prof. A. Prabhu for sparing the argon-ion laser and the LDV system, and the referees for their constructive comments.

References

1 TURNER, J S. — Turbulent entrainment: the development of entrainment assumptionand its application to geophysical flows, *J Fluid Mech*, 1986, **173**, 431–471

2 WARNER, J. — On steady-state one-dimensional models of cumulus convection, *J Atmos Sci*, 1970, **27**, 1035–1040.

3. PALUCH, I R. — The entrainment mechanism in *Colorado cumuli*, *J Atmos Sci.*, 1974, **36**, 2467–2478.

4. EMANUEL, K. A — *Atmospheric convection*, Ch. 7, pp. 199–206, 1994, Cambridge University Press.

5 BHAT, G. S, NARASIMHA, R. AND ARAKERI, V. H. — A new method of producing local enhancement of buoyancy in liquid flows, *Exp Fluids*, 1989, 7, 99–102

6. ELAVARASAN, R., BHAT, G. S, PRABHU, A. AND NARASIMHA, R. — An experimental study of a jet with local buoyancy enhancement, *Fluid Dyn. Res*, 1995, **16**, 187–202.

7. BHAT, G. S. AND NARASIMHA, R. — A volumetrically heated jet large eddy structure and entrainment characteristics, *J Fluid Mech*, 1996 (in press).

8. Fisher, H. B., List, E. J., Koh, R. C. Y., Imberger, J. and Brooks, N. H. *Mixing in inland and coastal waters*, 1979, Academic Press.

9. Koochesfahani, M. M. and Dimotakis, P. E. Laser induced measurements of concentration in a plane mixing layer, *AIAA 22nd Aerospace Meeting*, Reno, Nevada, 1984.

10. Papantoniou, D. and List, E. J. Large-scale structure in the far field of buoyant jets, *J. Fluid Mech.*, 1989, **209**, 151–190

11. Guilbault, G. C. *Practical fluorescence*, 1973, Marcel Dekker.

12. Walker, D. A. A fluorescence technique for measurement of concentration in mixing liquids, *J. Phys. E: Sci. Instrum.*, 1987, **20**, 217–224.

13. Durst, F., Melling, A. and Whitlaw, J. H. *Principles and practice of laser Doppler anemometry*, 1976, Academic Press.

14. Watrasiewicz, B. M. and Rudd, M. J. *Laser Doppler measurements*, 1976, Butterworth.

15. Drain, L. E. *The laser Doppler technique*, 1980, Wiley.

16. Broadwell, J. E. and Breidenthal, R. E. A simple model of mixing and chemical reaction in a turbulent shear flow, *J. Fluid Mech* , 1982, **125**, 397–410.

17. Dimotakis, P. E., Miakelye, R. C. and Papantoniou, D. A. Structure and dynamics of round turbulent jets, *Phys. Fluids*, 1983, **26**, 3185–3192.

18. Prabhu, A. and Narasimha, R. Equilibrium and relaxation in turbulent wakes, *J. Fluid Mech.*, 1972, **54**, 19–38.